

# **Introduction to Magnetic Nanoclusters**

***By: Adam Krause***

***Physics 672***

***2/24/07***

## ***I.) Nanoclusters: Quick Introduction***

Nanoclusters are mesoscopic particles ranging from several atoms to thousands of atoms in size. These particles are of interest because they can shed light on the transition from atomic properties to bulk material properties. By studying the properties of small clusters and working toward the larger ones, scientists can better understand the origins of known bulk material properties.

### **A.) A Few Types of Nanoclusters**

#### 1. Van der Waals Nanoclusters

Inert gas atoms form nanoclusters that are weakly bound by the Van der Waals force. The long-range atomic attraction is due to the induced dipole force. The short range repulsion is due to quantum closed shell electronic interactions and the binding energy per atom is less than 0.3 eV [1]. Echt, et al. [2] have shown experimentally that rare gases form Van der Waals clusters with icosahedral shapes as shown in *Figure 1*.

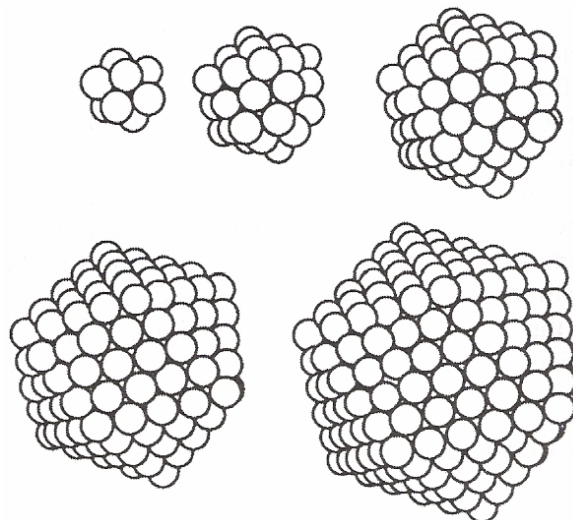


**Figure 1:** Van der Waals clusters are thought to form icosahedral shapes as shown here for different numbers of atoms. [1]

## 2. Ionic Nanocluster

These clusters are formed from ions attracted by the electrostatic force. NaCl is a typical example of an ionic cluster. The electrostatic bonds in ionic clusters are around 2-4 eV per atom. This is ten times as strong as the bond of a Van der Waals nanocluster [1]. *Figure 2* shows the crystal structure of NaCl.

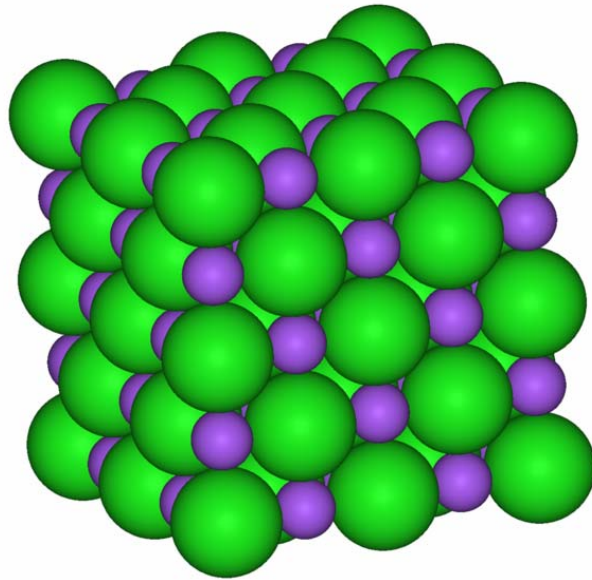


**Figure 2:** *The Crystal Structure of NaCl.*

Ionic clusters tend to be more stable if they have a completed cube shape. *Figure 3* shows the mass spectrum of NaI ionic clusters [3]. The peaks indicate a completed cube face. This indicates that completed cubes are more stable than partially completed cubes.

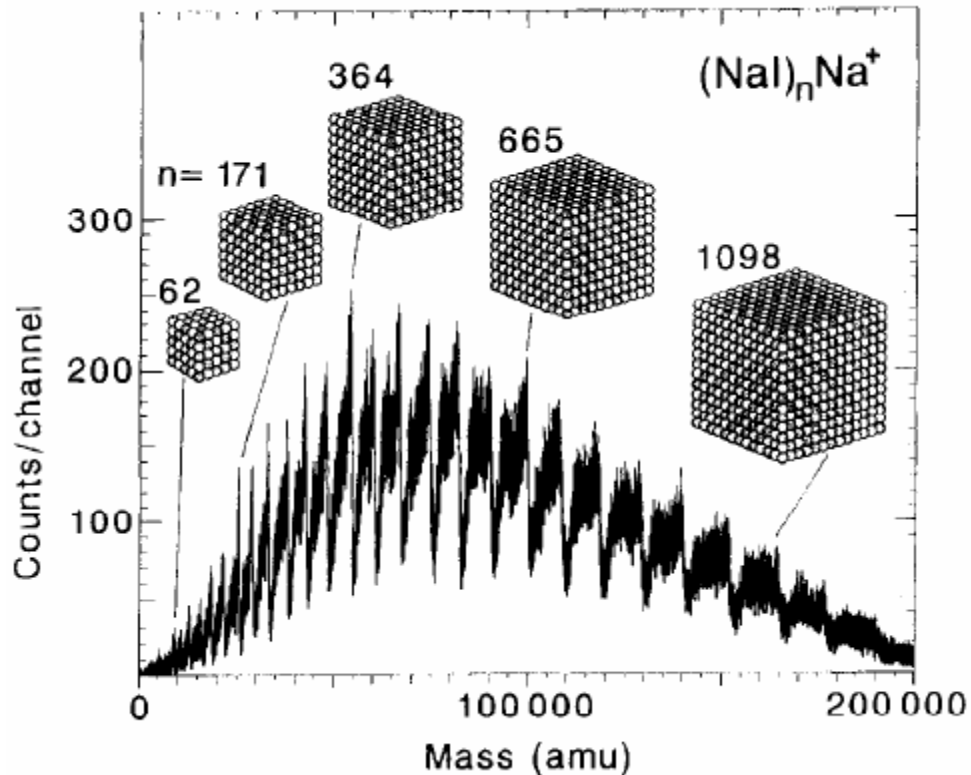


**Figure 3:** Mass spectrum of NaI ionic clusters. Every peak indicates a complete face of the cube. [3]

### 3. Metal Nanoclusters

Metal nanoclusters, the ones that are addressed in this paper, are more complicated in their bonding. Some metals bond primarily by the outer valence  $sp$  electrons. Others bond with the  $d$  orbitals below the valence orbitals. These  $d$  orbital materials, including Fe, Co, and Ni are the ones addressed below.

Because of the variation in bonds of metal clusters, the strength can vary from about 0.5 to 3 eV per atom [1].

## **II.) Description of Magnetic Particles**

This paper will focus on metal nanoclusters and their magnetic properties. First there will be a brief explanation of how magnetic nanoclusters are produced. Next, an explanation of the origins of cluster magnetism will be provided. Then

an example of a standard magnetic nanocluster experiment, the Stern-Gerlach experiment, will be explained. In the last three subsections the magnetic moment data of the nanoclusters will be discussed as well as the magnetic shell model.

### **A.) Production of Magnetic Nanoclusters**

The magnetic nanoclusters discussed below were formed using the laser vaporization technique first used by Dietz [4] and Bondybey [5]. This involves hitting a metal sample with a pulsed laser. Metal atoms evaporate off the sample surface and are cooled by a flow of inert gas. As they cool the atoms combine to form the metal nanoclusters. The nanoclusters are then expanded into a vacuum through a nozzle to further cool them. Though these nanoclusters vary in size, their sizes can be measured using a time-of-flight mass spectrometer as will be discussed in subsection **C**. The laser vaporization source used by Billas, et al. [6] is shown in *Figure 4*.

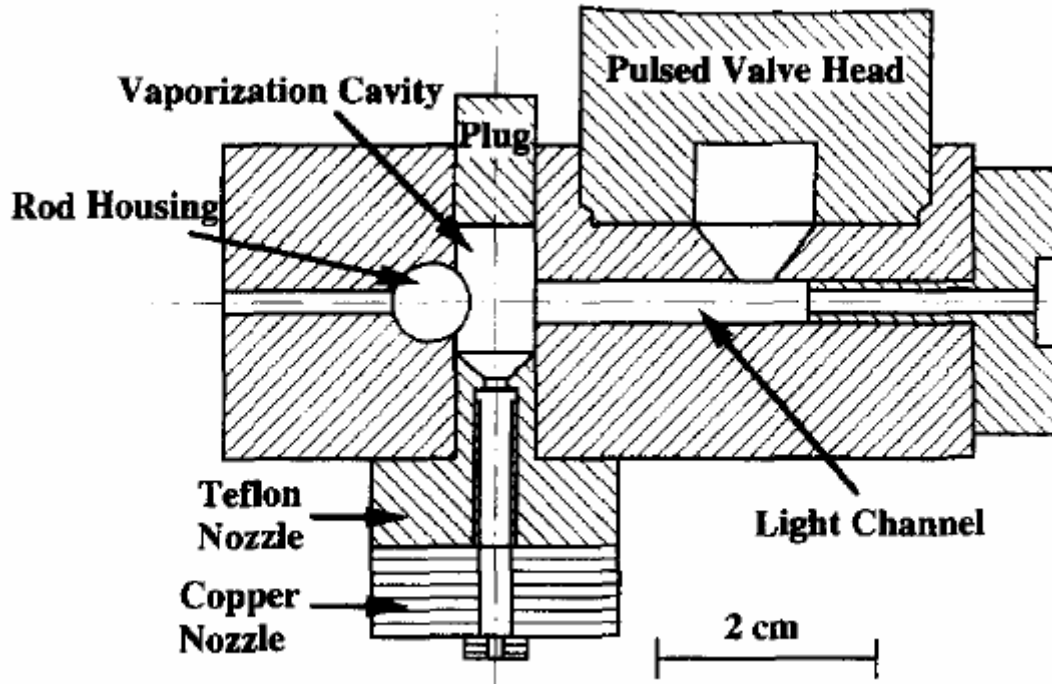


*Figure 4: The laser vaporization source used by Billas, et al. [6]. The pulsed laser beam strikes the metal rod and metal atoms evaporate. The atoms are cooled by the He flow to form the nanoclusters. The flow is then expanded through the copper nozzle into a vacuum to further cool the nanoclusters.*

## **B.) The Origin of Nanocluster Magnetic Moment**

Atomically speaking, magnetic moments arise from electron spin. Hund's Rules states that electrons tend to fill their orbitals in such a way as to maximize the net spin of the atom. This net electronic spin added to the orbital z-angular momentum is proportional to the magnetic moment of the atom. When these atoms combine to form nanoclusters, their magnetic moments can align to form a net magnetic moment for the nanocluster. The total magnetic moment for the nanocluster is not simply the sum of the individual atomic magnetic moments, especially in larger clusters where the total moment per atom is less than for smaller clusters. This is discussed in subsection **C** below.

### C.) Stern-Gerlach Experiment

The Stern-Gerlach experiment, shown in *Figure 5*, consists of a particle beam of nanoclusters passing through a non-uniform magnetic field. This non-uniform field couples with the magnetic moment of the nanoclusters and they are deflected. This deflection is a function of the particle mass and its magnetic moment. A time-of-flight mass spectrometer is then used to measure the mass of the particles [6, 7].

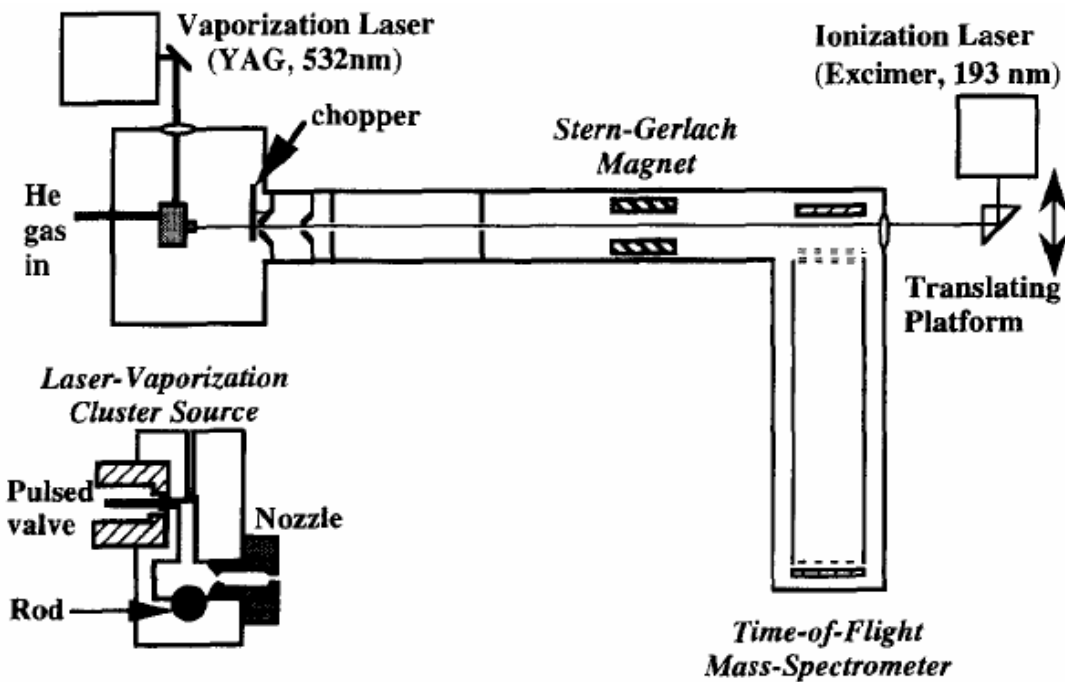


*Figure 5: Stern-Gerlach apparatus [6].*

### D.) Magnetic Moment vs. Cluster Size

The total magnetic moment of an atom is the z-angular momentum added to the spin of the atom. In particles of many atoms, the total magnetic moment is due to the atomic moments aligning themselves to create a net moment. These atomic magnetic moments do not simply add however. With increased

dimensionality (from atoms to surfaces to bulk) the atomic coordination number (basically the number of nearest neighbors) increases. In 3d metals, this increase in coordination number causes an overlapping of the 3d orbitals, those primarily responsible for the magnetic moment of the atom. This overlapping causes energy band structures to arise which tend to deplete the overall magnetic moment per atom of the material. *Figure 6* shows this transformation of the energy levels to energy bands as the material dimensionality is increased.

The overlapping 3d electrons are partially delocalized on the atoms which contribute to the mutual alignment of the magnetic moments [8]. This cohesive aligning of the magnetic moments gives ferromagnetic material its “frozen in” magnetic moment once it is removed from a magnetic field.

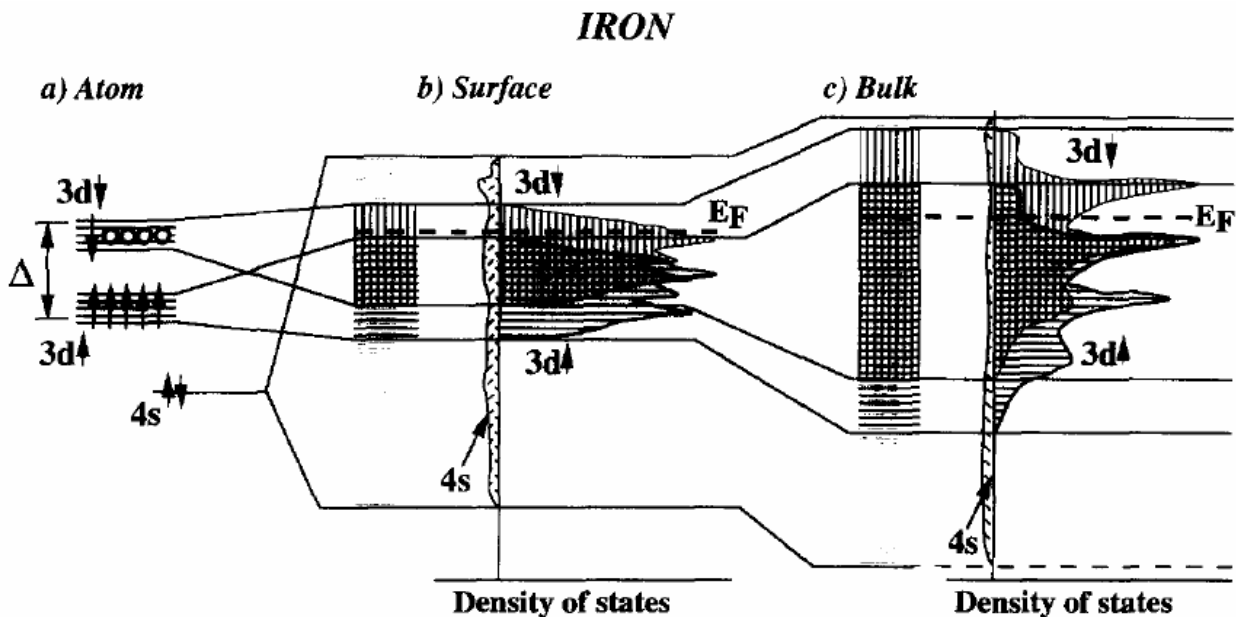


**Figure 6:** Theoretical band structure for a) Fe atom b) Fe surface c) Fe bulk [6].



In *Figure 6* the magnetic moment of the atom (*Figure 6a*) is simply the sum of the angular momentum and spin quantum numbers. This results in a large moment per atom ratio. As we increase dimensionality toward a surface (*Figure 6b*) and the orbitals begin to overlap and delocalize the exchange interaction causes some canceling of magnetic moments and the overall moment per atom is diminished. The extreme case of this is the bulk material (*Figure 6c*) which has the lowest magnetic moment per atom and the highest orbital overlap.

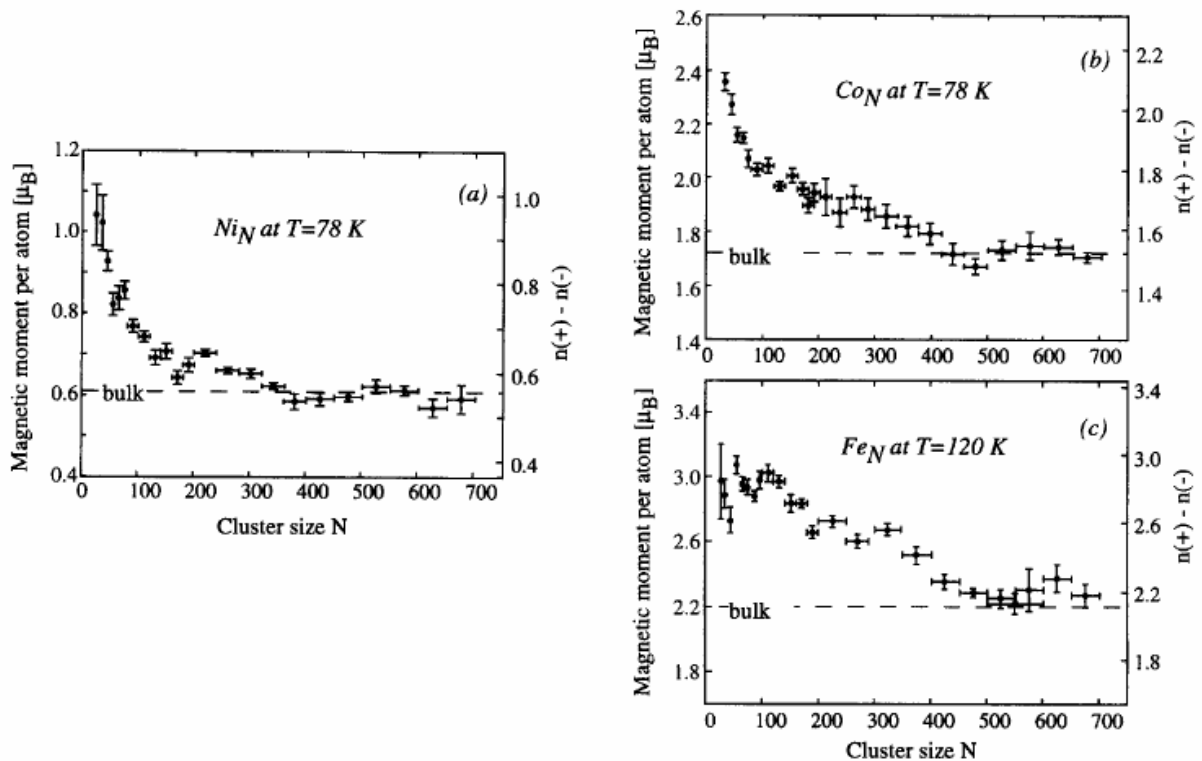


**Figure 7:** Magnetic moment vs. cluster size [6].

*Figure 7* shows this decrease in magnetic moment per atom for (a) Ni, (b) Co, and (c) Fe. It is interesting to note how the trends oscillate as they decrease. It has been proposed that this behavior is due to the atoms building into closed shell structures as they increase in size. In theory, every time a shell closes, the

magnetic moment reaches a minimum. This theory is explained in the next section.

### **E.) Magnetic Shell Model**

Jensen and Bennemann [9] propose a shell model by first assuming that the magnetic moment contribution of any atom depends on the “atomic environment” [9] at its lattice site. More exactly it depends on the number of nearest neighbors the atom has as well as the crystal structure of the cluster. As was stated above, the electronic orbitals become delocalized as the number of nearest neighbors increases and the inter-atomic spacing decreases. “The cluster is assumed to grow shell-by-shell, occupying subsequently sites of a b.c.c. or a f.c.c. lattice... The overall cluster shape is expected to resemble a cube, an octahedron, or a cubo-octahedron, i.e. regular shapes which minimize the surface energy.” [9]

The first step that Jensen and Bennemann took was to calculate the number of atoms in the closed shells of the f.c.c.-cube, f.c.c.-octahedron, f.c.c.-cubo-octahedron, b.c.c.-cube, and b.c.c.-octahedron. Then the experimental minima [8, 10] are compared to these numbers. This helps to determine which crystal structure most likely describes the nanocluster in question. The results of this investigation are shown in Table 1.

**Table 1:** Closed shell cluster size for various crystal structures. This is compared with cluster sizes at experimentally measured minima of the magnetic moment per atom on the right [8, 9, and 10].

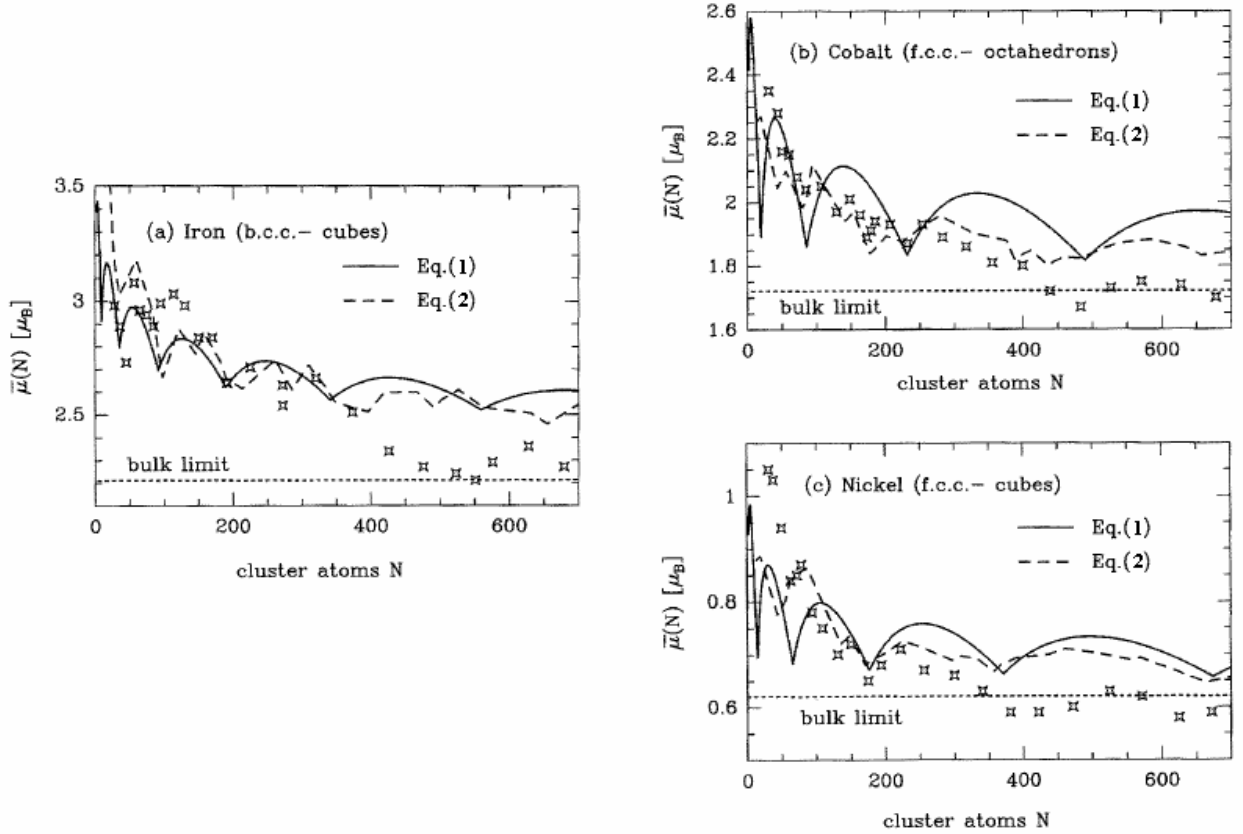
Shell n	Closed shell cluster size $N$					$N(\bar{\mu}_{\min})$		
	fcc- cube	fcc- oct.	fcc- c-o.	bcc- cube	bcc- oct.	Fe	Co	Ni
2'	43	43		15	27		50	
2	63	85	55	35	57	45	85	72
							129	
3'	140	165		59	89		173	131
3	172	231	147	91	143	85	232	175
4'	321	399		145	203	(150)	355	(260)
4	365	489	309	189	289	191	483	381
5'	610	777		285	385	273		625
5	666	891	561	341	511			
6'	1031	1331		491	651			
6	1099	1469	923	559	825	551		

Table 1 shows that for Fe clusters, the b.c.c.-cube fits the data. For f.c.c. cube calculations match up best with the Ni clusters. Finally, the Co cluster data is closest to the f.c.c.-octahedron calculations [9]. Using some approximations that will not be explained in this paper, Jensen and Bennemann found this equation for the magnetic moment per atom as a function of cluster size,  $N$  [9]:

$$\bar{\mu}(N) = \frac{N_0 \bar{\mu}_0 + N_1 \bar{\mu}_1 + N_{bulk} \mu_{bulk}}{x_0 N_0 + N_1 + N_{bulk}} \quad (1)$$

In this equation  $N_0$  and  $N_1$  are the number of atomic sites in the two outer most cluster shells. These numbers depend on the cluster shape which is why it is important to know that from the first step.  $N_{bulk}$  is the number of atomic sites in all the other shells. The numbers  $\mu_0$ ,  $\mu_1$ , and  $\mu_{bulk}$  are the magnetic moments per atom in the first shell, the second shell and the bulk respectively.  $x_0$  is the

statistical concentration of occupied sites in the outermost shell [9]. Equation 1 gives the oscillatory behavior seen in Figure 7. This behavior can be seen in Figure 8. The solid line shows the model given by Equation 1.



**Figure 8:** Shell model. The crosses are the measured data. The solid line is the model given by Equation 1. The dotted line is the model given by Equation 2. [8, 9, and 10].

An even better approximation comes from adding a further constraint on the values that  $\mu_i$  can take, where  $i$  is the lattice site. This constraint says that the magnetic moment at any given lattice site is a function of the number of nearest neighbors for that site. The conditions of this constraint look like this [9]:

$$\mu_i = \mu(q_i) = \begin{cases} \mu_1, q_i \leq q_c \\ \mu_2, q_i > q_c \end{cases} \quad (2)$$

The results of this further refinement are shown in *Figure 8* as the dotted line. It is obvious that this is not a perfect model, but that it does show the correct trend of minima.

## F.) Magnetic Moment vs. Temperature

It is also interesting to observe the magnetic moment of nanoclusters as it varies with temperature. *Figure 9* shows this data for Ni, Co, and Fe.

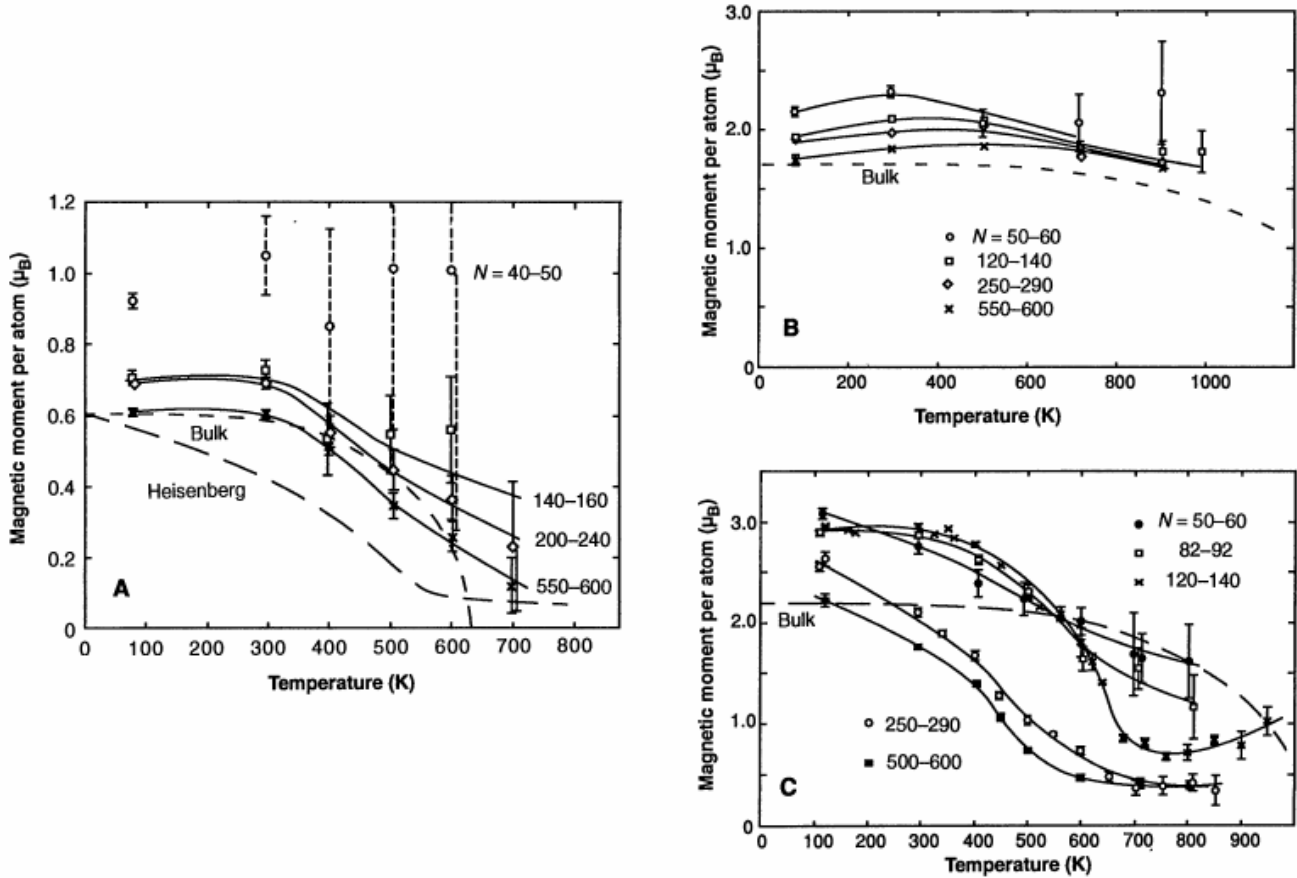


**Figure 9:** Magnetic moment vs. temperature for Ni (A), Co (B) and Fe (C) [8].

In *Figure 9(A)*, the larger Ni clusters approach the bulk limit for magnetic moment per atom as would be expected. The biggest difference from the bulk

trend is in the smooth transition downward as the nanocluster passes the Curie temperature. The bulk material drops sharply. This smooth transition can be explained and modeled by the Heisenberg model shown in *Figure 9(A)*. Binder et al. [11], calculated this behavior using Monte Carlo simulations. *Figure 10* shows an example of their simulation assuming a spherically shaped cluster.

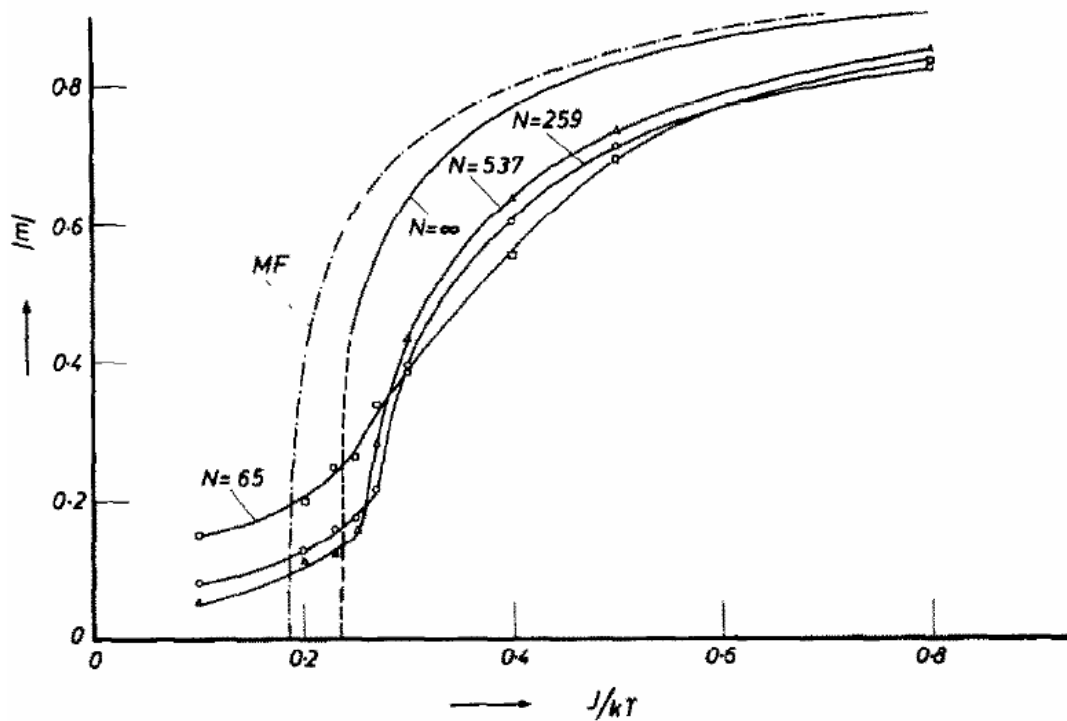


**Figure 10:** Simulation of magnetization of nanoclusters as a function of inverse temperature. The MF line is a calculation of an infinite system using Mean Field theory [11].

In the simulation in *Figure 10*, as the size of the nanocluster increases the transition at the Curie temperature sharpens just like the measured data. It seems that smaller particle maintain a magnetic order at higher temperatures than the bulk material [1].

Co, *Figure 9(B)*, also shows a trend toward the bulk as the cluster size increased. The only difference is a slight increase in magnetic moment per atom as the temperature increases. Bulk Co undergoes a phase change from *hcp* to *fcc* at 650 K. This may be the reason for the increase [8].

Fe shows an entirely different trend than the other two metals in *Figure 9(C)*. It does not follow that bulk trend. This difference may be attributable to a phase transition in Fe from a *bcc* to an *fcc* configuration that occurs in bulk Fe at 1150 K [8].

### ***III.) Superparamagnetism***

Most bulk magnetic materials exhibit ferromagnetic behavior below the Curie temperature and paramagnetic behavior above the Curie temperature. However, when the particle being considered is sufficiently small, some materials that are normally ferromagnetic behave paramagnetic even below the Curie temperature. This phenomenon is called superparamagnetism. It is the tendency of the particle to lose its net magnetic moment due to ambient thermal conditions randomly reorienting the spins of the particle after it is removed from a magnetic field thereby destroying the net magnetic moment. This is not contrary to the above data showing the ferromagnetic tails in *Figures 9 and 10* because, as is explained by Billas [10], the superparamagnetic model is limited due to rotational effects when the clusters are expanded and cooled. The iron clusters in this study by Jackson et al. are embedded in a silver matrix.

Jackson et al. measured the magnetization loops of Fe nanoclusters for a few temperatures between 5 K and 50 K [12]. This data is shown in *Figure 11* as a function of the applied B-field /temperature.

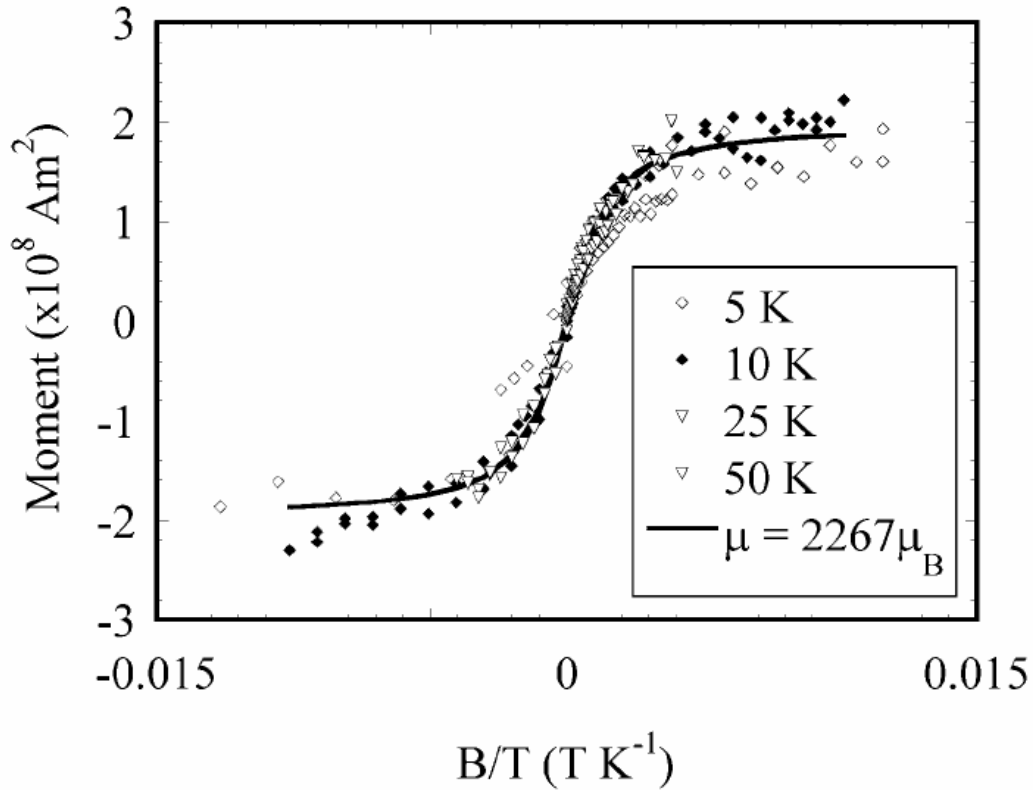


**Figure 11:** The magnetization loops of Fe nanoclusters as a function of  $B/T$ . Only the 5 K loop shows no definite signs of superparamagnetism. All the others show the effect. The solid line is a 10 K Langevin function prediction which will not be discussed in this paper [12].

The data in *Figure 11* was taken using a SQUID magnetometer. The magnetization loop for the 5 K Fe nanoclusters shows a broadening as the B-field is changed. This behavior is hysteresis and is a clear indicator of ferromagnetism. Therefore at 5 K, the Fe clusters do not show superparamagnetic behavior. The other temperatures do not show hysteresis. Therefore they are indeed superparamagnetic.



#### ***IV.) Conclusion***

This paper briefly explains the experiments done on and the phenomena observed with magnetic metal nanoclusters. It was shown that materials that are macroscopically magnetic, behave differently on the nanometer scale. Among these observations is that of superparamagnetism. This is a particularly interesting phenomenon because it presents a problem when using nanoclusters for electronic memory applications. Time relaxation of the cluster magnetic moment due to superparamagnetism would destroy the memory bit that the cluster holds. As also shown above, larger clusters behave ferromagnetically as is required by data storage. This puts a theoretical minimum on the size of memory storage bits used in electronics. Further research into magnetic nanoclusters may resolve this problem.

#### **IV.) References**

1. Alonso, J. A., Structure and Properties of Atomic Nanoclusters (Imperial College Press, London, 2005).
2. Echt, O., et al., *J. Chem. Soc. Faraday Trans.*, 86 (1990) 2411
3. Martin, T. P., *Physics Reports*, 273 (1996) 199
4. Dietz, T. G., et al., *J. Chem. Phys.*, 74 (1981) 6511
5. Bondybey, V. E., and J. H. English, *J. Chem. Phys.*, 76 (1982) 2165
6. Billas, M. L., A. Chatelain, and W. A. de Heer, *J. Magn. Magn. Mater.* 168 (1997) 64
7. Cox, D. M., et al, *Phys. Rev. B.*, 32 (1985) 7291
8. Billas, M. L., A. Chatelain, and W. A. de Heer, *Science* 265 (1994) 1682
9. Jensen, P. J., and K. H. Bennemann, *Z. Phys. D.* 35 (1995) 273
10. Billas, M. L., et al., *Phys. Rev. Lett.*, 71 (1993) 4067
11. Binder, K., et al., *J. Phys. Chem. Solids*, 31 (1970) 391
12. Jackson, T. J., et al., *J. Phys.: Condens. Matter*, 12 (2000) 1399